TOWARDS NUMERICAL TWO-LOOP INTEGRAND REDUCTION

Costas G. Papadopoulos

in collaboration with G. Bevilacqua, D. Canko, A. Spourdalakis

INPP, NCSR "Demokritos", 15310 Athens, Greece





Torino HOCTools-II mini-workshop, October 23, 2025

OUTLINE

- DS recursive equations
- Review of the OPP approach
- Constructing the 2-loop integrand
- Integrand reduction
- Summary & Outlook

 \rightarrow LO & AO

 $\rightarrow \mathsf{NLO}$

 $\rightarrow NNLO$

 \rightarrow NNLO

THE PRECISION ADVENTURE

DS recursive equations

How to avoid Feynman diagrams

 \rightarrow a highly subjective point of view

LO - Dyson-Schwinger Recursive Equations

From Feynman Diagrams to recursive equations: taming the n!

• 1999 HELAC: The first code to calculate recursively tree-order amplitudes for (practically) arbitrary number of particles

→A. Kanaki and C. G. Papadopoulos, Comput. Phys. Commun. 132 (2000) 306 [arXiv:hep-ph/0002082].

→F. A. Berends and W. T. Giele, Nucl. Phys. B 306 (1988) 759.

→ F. Caravaglios and M. Moretti, Phys. Lett. B 358 (1995) 332.

Unfortunately not so much on the second line !

→Integrals and Integrands

TAMING THE BEAST ...

From Feynman graphs ...

to Dyson-Schwinger recursion! Helac-Phegas

$$gg \rightarrow ng$$
 2 3 4 5 6 7 8 9 $\#$ 5 15 35 70 126 210 330 495

Beyond Tree-order

NLO

Don't make integrals, make integrands !

The one loop paradigm

basis of scalar integrals:

known already before NLO-R; remember this is not the case for higher orders

→G. 't Hooft and M. J. G. Veltman, Nucl. Phys. B 153 (1979) 365.

→ Z. Bern, L. J. Dixon and D. A. Kosower, Nucl. Phys. B 412 (1994) 751

→G. Passarino and M. J. G. Veltman, Nucl. Phys. B **160** (1979) 151.

→Z. Bern, L. J. Dixon, D. C. Dunbar and D. A. Kosower, Nucl. Phys. B 425 (1994) 217.

$$\mathcal{A} = \sum_{I \subset \{0,1,\cdots,m-1\}} \int \frac{\mu^{(4-d)} d^d \bar{q}}{(2\pi)^d} \frac{\bar{N}_I(\bar{q})}{\prod_{i \in I} \bar{D}_i(\bar{q})}$$

$$A = \sum d_{i_1 i_2 i_3 i_4} + \sum c_{i_1 i_2 i_3} + \sum b_{i_1 i_2} + \sum a_{i_1} + \sum a_{i_1}$$

 $a, b, c, d \rightarrow \text{cut-constructible part}$

 $R \rightarrow \text{rational terms}$

THE OLD "MASTER" FORMULA

$$\mathcal{A} \to \int \frac{\bar{N}(\bar{q})}{\bar{D}_0 \bar{D}_1 \cdots \bar{D}_{m-1}} = \sum_{i_0 < i_1 < i_2 < i_3}^{m-1} d(i_0 i_1 i_2 i_3) \int \frac{1}{\bar{D}_{i0} \bar{D}_{i1} \bar{D}_{i2} \bar{D}_{i2}}$$

$$+ \sum_{i_0 < i_1 < i_2}^{m-1} c(i_0 i_1 i_2) \int \frac{1}{\bar{D}_{i0} \bar{D}_{i1} \bar{D}_{i2}}$$

$$+ \sum_{i_0 < i_1}^{m-1} b(i_0 i_1) \int \frac{1}{\bar{D}_{i0} \bar{D}_{i1}}$$

$$+ \sum_{i_0}^{m-1} a(i_0) \int \frac{1}{\bar{D}_{i0}}$$

$$+ \text{ rational terms}$$

OPP "MASTER" FORMULA - I

General expression for the 4-dim N(q) at the integrand level in terms of D_i

 $\rightarrow \mathsf{G.\ Ossola,\ C.\ G.\ Papadopoulos\ and\ R.\ Pittau,\ [arXiv:hep-ph/0609007\ [hep-ph]].}$

$$N(q) = \sum_{i_{0} < i_{1} < i_{2} < i_{3}}^{m-1} \left[d(i_{0}i_{1}i_{2}i_{3}) + \tilde{d}(q; i_{0}i_{1}i_{2}i_{3}) \right] \prod_{i \neq i_{0}, i_{1}, i_{2}, i_{3}}^{m-1} D_{i}$$

$$+ \sum_{i_{0} < i_{1} < i_{2}}^{m-1} \left[c(i_{0}i_{1}i_{2}) + \tilde{c}(q; i_{0}i_{1}i_{2}) \right] \prod_{i \neq i_{0}, i_{1}, i_{2}}^{m-1} D_{i}$$

$$+ \sum_{i_{0} < i_{1}}^{m-1} \left[b(i_{0}i_{1}) + \tilde{b}(q; i_{0}i_{1}) \right] \prod_{i \neq i_{0}, i_{1}}^{m-1} D_{i}$$

$$+ \sum_{i_{0}}^{m-1} \left[a(i_{0}) + \tilde{a}(q; i_{0}) \right] \prod_{i \neq i_{0}}^{m-1} D_{i}$$

→G. Ossola, C. G. Papadopoulos and R. Pittau, JHEP 05 (2008), 004 [arXiv:0802.1876 [hep-ph]].

$$ar{D}_i = (ar{q} + p_i)^2 - m_i^2 \,, \quad p_0
eq 0 \,,$$
 $ar{D}_i = D_i + ilde{q}^2$ $m_i^2
ightarrow m_i^2 - ilde{q}^2 .$

$$d(ijkl; \tilde{q}^{2}) = d(ijkl) + \tilde{q}^{2}d^{(2)}(ijkl) + \tilde{q}^{4}d^{(4)}(ijkl),$$

$$c(ijk; \tilde{q}^{2}) = c(ijk) + \tilde{q}^{2}c^{(2)}(ijk),$$

$$b(ij; \tilde{q}^{2}) = b(ij) + \tilde{q}^{2}b^{(2)}(ij).$$



$$d^{(4)}(ijkl) = \lim_{\tilde{q}^2 \to \infty} \frac{d(ijkl; \tilde{q}^2)}{\tilde{q}^4},$$

$$c^{(2)}(ijk) = \lim_{\tilde{q}^2 \to \infty} \frac{c(ijk; \tilde{q}^2)}{\tilde{q}^2},$$

$$b^{(2)}(ij) = \lim_{\tilde{q}^2 \to \infty} \frac{b(ij; \tilde{q}^2)}{\tilde{q}^2},$$

$$d^{(4)}(ijkl) = \frac{d(ijkl; 1) + d(ijkl; -1) - 2d(ijkl)}{2}$$

$$c^{(2)}(ijk) = c(ijk; 1) - c(ijk),$$

$$b^{(2)}(ij) = b(ij; 1) - b(ij).$$

$$\int d^{n}\bar{q} \frac{\tilde{q}^{4}}{\bar{D}_{i}\bar{D}_{j}\bar{D}_{k}\bar{D}_{l}} = -\frac{i\pi^{2}}{6} + \mathcal{O}(\epsilon),$$

$$\int d^{n}\bar{q} \frac{\tilde{q}^{2}}{\bar{D}_{i}\bar{D}_{j}\bar{D}_{k}} = -\frac{i\pi^{2}}{2} + \mathcal{O}(\epsilon),$$

$$\int d^{n}\bar{q} \frac{\tilde{q}^{2}}{\bar{D}_{i}\bar{D}_{j}} = -\frac{i\pi^{2}}{2} \left[m_{i}^{2} + m_{j}^{2} - \frac{(p_{i} - p_{j})^{2}}{3} \right] + \mathcal{O}(\epsilon).$$

$$R_{1} = -\frac{i}{96\pi^{2}}d^{(2m-4)} - \frac{i}{32\pi^{2}}\sum_{i_{0}< i_{1}< i_{2}}^{m-1}c^{(2)}(i_{0}i_{1}i_{2})$$

$$- \frac{i}{32\pi^{2}}\sum_{i_{0}< i_{1}}^{m-1}b^{(2)}(i_{0}i_{1})\left(m_{i_{0}}^{2} + m_{i_{1}}^{2} - \frac{(p_{i_{0}} - p_{i_{1}})^{2}}{3}\right).$$

→P. Draggiotis, M. V. Garzelli, C. G. Papadopoulos and R. Pittau, JHEP 04 (2009), 072 [arXiv:0903.0356 [hep-ph]].

 \rightarrow M. V. Garzelli, I. Malamos and R. Pittau, JHEP **01** (2010), 040 [erratum: JHEP **10** (2010), 097]

$$\bar{N}(\bar{q}) = N(q) + \tilde{N}(\tilde{q}^2, q, \epsilon).$$

$$egin{array}{lll} ar{q} &=& q+ ilde{q}\,, \ ar{\gamma}_{ar{\mu}} &=& \gamma_{\mu}+ ilde{\gamma}_{ar{\mu}}\,, \ ar{g}^{ar{\mu}ar{
u}} &=& g^{\mu
u}+ ilde{g}^{ ilde{\mu} ilde{
u}}\,. \end{array}$$

$$\mathrm{R}_2 \equiv rac{1}{(2\pi)^4} \int d^n\, ar{q} rac{ ilde{N}(ilde{q}^2,q,\epsilon)}{ar{D}_0ar{D}_1\cdotsar{D}_{m-1}} \equiv rac{1}{(2\pi)^4} \int d^n\, ar{q}\, \mathcal{R}_2\,.$$



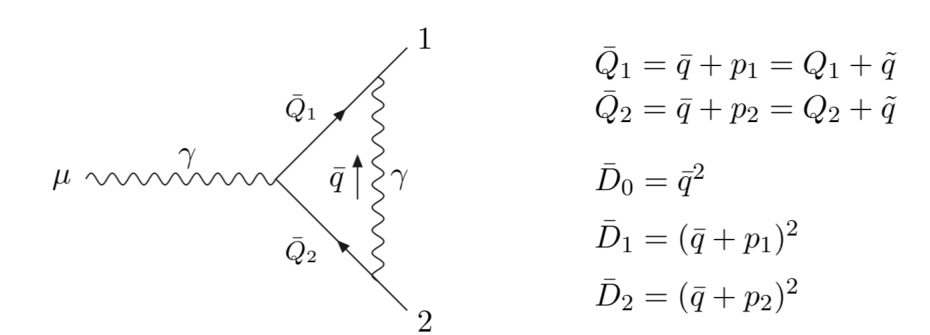


Figure 1: QED γe^+e^- diagram in n dimensions.

 $\epsilon\text{-dimensional }\gamma$ matrices freely anti-commute with four-dimensional ones: $\{\gamma_\mu,\tilde{\gamma}_\nu\}\ =0$

$$\begin{split} \bar{N}(\bar{q}) & \equiv e^3 \left\{ \bar{\gamma}_{\bar{\beta}} \left(\bar{Q}_1 + m_e \right) \gamma_{\mu} \left(\bar{Q}_2 + m_e \right) \bar{\gamma}^{\bar{\beta}} \right\} \\ & = e^3 \left\{ \gamma_{\beta} (Q_1 + m_e) \gamma_{\mu} (Q_2 + m_e) \gamma^{\beta} \right. \\ & - \epsilon \left(Q_1 - m_e \right) \gamma_{\mu} (Q_2 - m_e) + \epsilon \tilde{q}^2 \gamma_{\mu} - \tilde{q}^2 \gamma_{\beta} \gamma_{\mu} \gamma^{\beta} \right\} \,, \end{split}$$

$$\int d^n \bar{q} \frac{\tilde{q}^2}{\bar{D}_0 \bar{D}_1 \bar{D}_2} = -\frac{i\pi^2}{2} + \mathcal{O}(\epsilon),$$

$$\int d^n \bar{q} \frac{q_\mu q_\nu}{\bar{D}_0 \bar{D}_1 \bar{D}_2} = -\frac{i\pi^2}{2\epsilon} g_{\mu\nu} + \mathcal{O}(1),$$

gives

$$R_2 = -\frac{ie^3}{8\pi^2}\gamma_\mu + \mathcal{O}(\epsilon),$$



Computing 1PI contributions to $R_2 o R_2$ for any 1-loop amplitude R_2 vertices in full analogy with renormalization CT

OPP@work

- Determining the on-shell momenta through $D_i = 0$ and computing all coefficients.
- ② Determining the on-shell momenta through $D_i = \mu$ and μ dependence of certain coefficients, namely R_1 .
- ① Using new Feynman rules to compute with tree-like DS the rest of R contribution, namely R_2 .

```
→ G. Ossola, C. G. Papadopoulos and R. Pittau, [arXiv:0802.1876 [hep-ph]].
```

 \rightarrow M. V. Garzelli, I. Malamos and R. Pittau, [arXiv:0910.3130 [hep-ph]].

Towards higher precision:

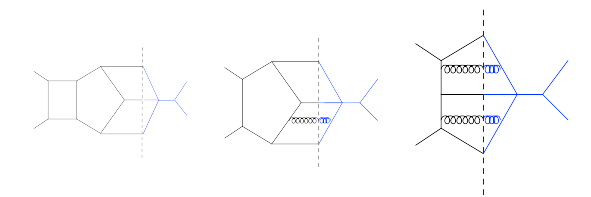
NNLO and beyond

I have a dream ...

PERTURBATIVE QCD AT NNLO

What do we need for an NNLO calculation?

$$p_1, p_2 \rightarrow p_3, ..., p_{m+2}$$



PERTURBATIVE QCD AT NNLO

What do we need for an NNLO calculation?

$$\sigma_{NNLO} \rightarrow \int_{m} d\Phi_{m} \left(2Re(M_{m}^{(0)*}M_{m}^{(2)}) + \left| M_{m}^{(1)} \right|^{2} \right) J_{m}(\Phi) \qquad VV$$

$$+ \int_{m+1} d\Phi_{m+1} \left(2Re\left(M_{m+1}^{(0)*}M_{m+1}^{(1)} \right) \right) J_{m+1}(\Phi) \qquad RV$$

$$+ \int_{m+2} d\Phi_{m+2} \left| M_{m+2}^{(0)} \right|^{2} J_{m+2}(\Phi) \qquad RR$$

 $RV + RR \rightarrow$ antenna-S, colorfull-NNLO, sector-improved residue subtraction, nested soft-collinear, local analytic sector subtraction, projection to born, q_T , N-jetiness

```
ightarrow A. Gehrmann-De Ridder, T. Gehrmann and M. Ritzmann, JHEP 1210 (2012) 047 
ightarrow P. Bolzoni, G. Somogyi and Z. Trocsanyi, JHEP 1101 (2011) 059
```

→ M. Czakon and D. Heymes, Nucl. Phys. B **890** (2014) 152

→S. Catani and M. Grazzini, Phys. Rev. Lett. **98** (2007) 222002 → R. Boughezal, C. Focke, X. Liu and F. Petriello, Phys. Rev. Lett. **115** (2015) no.6, 062002

→ M. Cacciari, F. A. Dreyer, A. Karlberg, G. P. Salam and G. Zanderighi, Phys. Rev. Lett. 115, no. 8, 082002 (2015)

→ F. Caola, K. Melnikov and R. Röntsch, Eur. Phys. J. C 77, no. 4, 248 (2017)

→ F. Caoia, K. Meinikov and R. Kontsch, Eur. Phys. J. C 11, no. 4, 248 (2017)

→ L. Magnea, E. Maina, G. Pelliccioli, C. Signorile-Signorile, P. Torrielli and S. Uccirati, arXiv:1806.09570 [hep-ph].

AMPLITUDE CONSTRUCTION

Amplitude construction

AMPLITUDE CONSTRUCTION

- ullet Standard approach: QGRAF o symbolic manipulation, dimensionally regularized amplitudes o IBP: FIRE, Kira or numerical pySecDec
- Numerical unitarity \to dimensionally regularized amplitudes by gluing tree amplitudes in different integer dimensions $\to D_s$

```
→ S. Abreu, J. Dormans, F. Febres Cordero, H. Ita, M. Kraus, B. Page, E. Pascual, M. S. Ruf and V. Sotnikov, CPC 267 (2021), 108069
```

ullet OpenLoops o Feynman graph o opening the loops o amplitudes in d=4 o coefficients of tensor integrals

```
\rightarrow S. Pozzorini, N. Schär and M. F. Zoller, [arXiv:2201.11615 [hep-ph]].
```

 \rightarrow talk by Max Zoller

HELAC COLOR TREATMENT

Colour flow or colour connection representation

$$\mathcal{M}_{j_2,\dots,j_k}^{\mathsf{a}_1,i_2,\dots,i_k} t_{\mathsf{i}_1\mathsf{j}_1}^{\mathsf{a}_1} \to \mathcal{M}_{j_1,j_2,\dots,j_k}^{i_1,i_2,\dots,i_k}$$

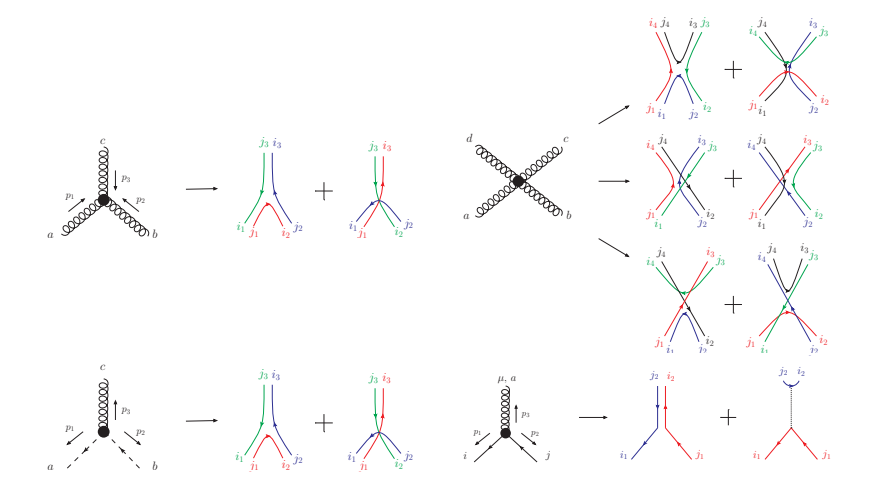
$$\mathcal{M}_{j_1,j_2,\ldots,j_k}^{i_1,i_2,\ldots,i_k} = \sum_{\sigma} \delta_{i_{\sigma_1},j_1} \delta_{i_{\sigma_2},j_2} \ldots \delta_{i_{\sigma_k},j_k} A_{\sigma} \to \mathsf{n!}$$

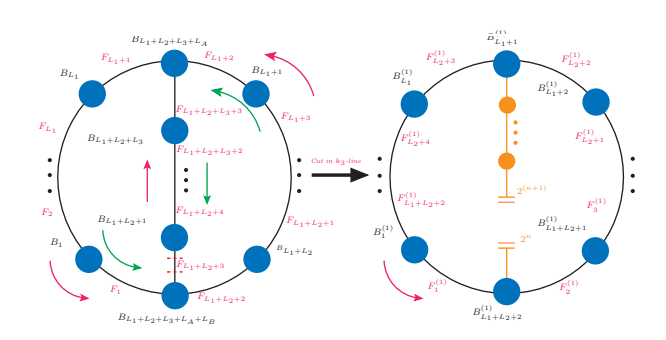
gluons, ghosts o (i,j), quark o (i,0), anti-quark o (0,j), other o (0,0)

$$\sum_{\sigma,\sigma'} A_{\sigma}^* \mathcal{C}_{\sigma,\sigma'} A_{\sigma'}$$

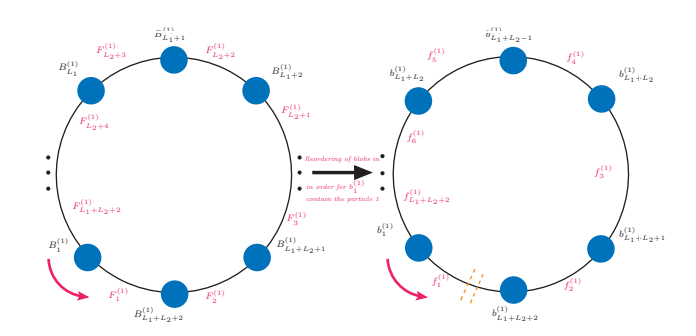
$$C_{\sigma,\sigma'} \equiv \sum_{\{i\},\{j\}} \delta_{i_{\sigma_1},j_1} \delta_{i_{\sigma_2},j_2} \dots \delta_{i_{\sigma_k},j_k} \delta_{i_{\sigma'_1},j_1} \delta_{i_{\sigma'_2},j_2} \dots \delta_{i_{\sigma'_k},j_k} = N_c^{m(\sigma,\sigma')}$$

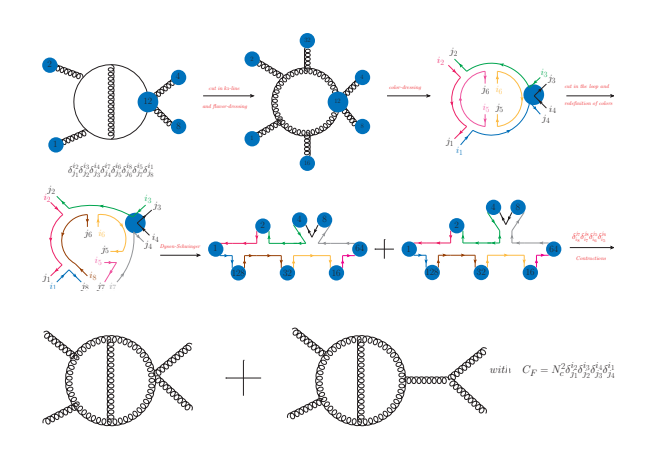
Colour-flow Feynman rules





HELAC2LOOP@work





INFO INFO	NUM	1		110	of			33	2			7						
	===			=====		====		====	===:	===								
INFO	4	80	35	9	1	1	16	35	5	64	35	7	0	0	0	0	1	2
INFO	4	12	35	10	1	1	4	35	3	8	35	4	0	0	0	0	1	1
INFO	4	92	35	11	1	2	12	35	10	80	35	9	0	0	0	0	1	1
INFO	5	92	35	11	2	2	4	35	3	8	35	4	80	35	9	0	1	5
INFO	4	124	35	12	1	1	32	35	6	92	35	11	0	0	0	0	1	2
INFO	4	126	35	13	1	1	2	35	2	124	35	12	0	0	0	0	1	1
INFO	4	254	35	14	1	1	128	35	8	126	35	13	0	0	0	0	1	2
INFO	6	1	12	1	2	12	35	35	35	35	35	35	0	0	0	0	5	9

Remark: Skeleton knows nothing about d: it can be used in d=4 or any other dimension including $d=4-2\epsilon$; symbolic output also possible.



Process	#	Loop-Flavors	Color	Size	Crea. Time	Nums
gg o gg	2	$\{g,c,ar{c}\}$	Lead.	8.9 MB	15.017s	4560
gg o gg	2	$\{g,q,\overline{q},c,\overline{c}\}$	Full	110.6 MB	6m 54.574s	89392
gg o qar q	2	$\{g,q,\bar{q},c,\bar{c}\}$	Full	16.1 MB	3m 14.509s	13856
gg o ggg	2	$\{g,c,\bar{c}\}$	Lead.	300.0 MB	21m 42.609s	81480
$gg o qar{q}g$	2	$\{g,q,\overline{q},c,\overline{c}\}$	Full	686.1 MB	400m 31.591s	318964
gg o gg	1	$\{g,q,\overline{q},c,\overline{c}\}$	Full	537.8 kB	2.386s	768
gg o ggg	1	$\{g,q,\bar{q},c,\bar{c}\}$	Full	15.1 MB	8m 53.349s	11496
gg o gggg	1	$\{g,c,\bar{c}\}$	Lead.	394.0 MB	104m 14.95s	19680

TABLE: Table containing information for the skeleton of some QCD processes at one- and two-loop. Therein, the column # refers to the number of loops, *Loop-Flavors* denotes the flavor of the particles included in the loops, and *Color* indicates the color order, with Lead. and Full referring to leading- and full-color approximation, respectively. The columns *Size* and *Crea.Time*, indicate the size of the skeleton and the real-time consumed for its construction, respectively. The last column (*Nums*) signifies the number of separate contributions (numerators) to the amplitude. These results have been obtained running 1-core on a laptop (i7 processor, 8-core, 24GB RAM).

Integrand reduction

 $\rightarrow \ Bevilacqua, \ Giuseppe \ and \ Canko, \ Dhimiter \ and \ Papadopoulos, \ Costas \ and \ Spourdalakis, \ Aris,, \ hep-ph: \ 2506.07231$

→ Talk in GGI 2024: → click to link

$$\mathcal{A}^{(L)}(\{p\}) = \sum_{g=1}^G \left(\int \prod_{i=1}^L \left[dk_i \right] \frac{\mathcal{N}(k_1, \dots, k_L, \{p\})}{D_1 D_2 \cdots D_n} \right)_g,$$

Extending the OPP approach to two loops, one can express the numerator $\mathcal N$ of a generic two-loop integrand in the following form:

$$\mathcal{N} = P^{(n)} + \sum_{i=1}^{n} P_i^{(n-1)} D_i + \sum_{i=1}^{n-1} \sum_{i>i}^{n} P_{ij}^{(n-2)} D_i D_j + \ldots + P_{12...n}^{(0)} D_1 D_2 \ldots D_n$$

A generic 2-loop integrand can be written using the following scalar product set:

$$\{p_i\cdot p_j,\,k_i\cdot k_j,\,k_i\cdot p_j,\,k_i\cdot \eta_j\}$$

$$P = \sum_{l=1}^{M} b_l m_l, \tag{1}$$

where $b_i = b_i(\{p\})$ are coefficients which depend on the external kinematics, and the monomials m_i are built upon the ISP characteristic of each term.

Focusing on the two-loop case, our goal is to decompose the amplitude, $\mathcal{A}^{(2)}$, in terms of a set of Feynman integrals F_i and coefficients c_i that depend only on the external kinematics,

$$A^{(2)} = \sum_{i} c_i(\{p\}) F_i , \qquad (2)$$

where the F_i 's take the form

$$F_i \equiv F(a_1, \ldots, a_N) = \int \prod_{i=1}^2 [dk_i] \frac{1}{D_1^{a_1} \ldots D_N^{a_N}}, \quad a_i \in \mathbb{Z}.$$
 (3)

ightarrow V. Sotnikov, Thesis

This can be achieved by appropriately expressing the monomials m_l in Eq. (1) in terms of the inverse propagators D_l . Eq. (2) is at the core of *numerical* methods for two-loop computations. Provided that the integrals F_l are known (or a procedure to reduce the latter to a subset of master integrals is established), determining the coefficients c_l at *integrand level* helps to address the problem of two-loop computations in a general, process-independent way. This idea expands upon well-established methods developed for one-loop calculations, such as OPP reduction.

Linear fit and fit by cut approach

$$D_1 = D_2 = \ldots = D_n = 0$$
, (4)

we can identify the coefficients of $P^{(n)}$,

$$P^{(n)} = \mathcal{N}|_{D_1 = D_2 = \dots = D_n = 0}. \tag{5}$$

Then we can iteratively fit the rest of the polynomials by appropriately subtracting the terms computed in the previous step. For instance, the first next-to-maximal contribution reads

$$P_1^{(n-1)} = \left. \left(\frac{\mathcal{N} - \mathcal{N}|_{D_1 = D_2 = \dots = D_n = 0}}{D_1} \right) \right|_{D_2 = \dots = D_n = 0}, \tag{6}$$

and so on. We note that cut equations, Eq. (4), translate into a system of linear relations among scalar products $k_i \cdot k_j$ and $k_i \cdot p_j$, where k_i and p_j denote generically loop and external momenta, respectively. This allows us to straightforwardly solve Eq. (5), Eq. (6), and the rest of the equations resulting from all the sub-maximal cuts, by substitution rules, for any process. We call this procedure of solving Eq. (1), a linear fit. We will show in the following sections how this applies to the case of 4-, 5-, and 6-particle scattering amplitudes.

In certain instances, the analytical calculation of the numerator $\mathcal N$ can prove to be a highly challenging task. In such cases, resorting to a numerical computation, facilitated by dedicated software packages such as HELAC-2L00P, can be a feasible alternative. In this case, there are two issues to be addressed:

→ Canko, Dhimiter and Bevilacqua, Giuseppe and Papadopoulos, Costas, hep-ph:2309.14886

the solutions of cut equations must be expressed in a form suitable for numerical evaluation of numerators;

2 the polynomials P appearing in Eq. (1) must be constructed without a priori analytical knowledge of the numerator.

To address the first issue, we need a suitable representation of the loop momenta. Given two arbitrary massless momenta l_1^{μ} , l_2^{μ} , let us define

$$l_{\perp}^{\mu} = \bar{u}_{-}(l_{1})\gamma^{\mu}u_{-}(l_{2}),$$

 $l_{\perp}^{\mu} = \bar{u}_{-}(l_{2})\gamma^{\mu}u_{-}(l_{1}).$ (7)

The set $\{l_1^\mu, l_2^\mu, l_3^\mu, l_4^\mu\}$ forms a basis in d=4 dimensions. This allows us to express the loop momenta k_1, k_2 as follows,

$$k_1 = x_1 \int_1^{(1)} + x_2 \int_2^{(1)} + x_3 \int_3^{(1)} + x_4 \int_4^{(1)} k_2 = y_1 \int_1^{(2)} + y_2 \int_2^{(2)} + y_3 \int_3^{(2)} + y_4 \int_4^{(2)}$$
(8)

where the coefficients x_i and y_i are expressible in terms of scalar products of the form $k_i \cdot p_j$. The latter coefficients characterize the loop momenta in d=4 dimensions. Complemented by μ_{11} , μ_{12} and μ_{22} , they form a set of eleven variables which characterizes completely the loop momenta in $d=4-2\epsilon$ dimensions: $\vec{X}=\{x_1,x_2,x_3,x_4,y_1,y_2,y_3,y_4,\mu_{11},\mu_{12},\mu_{22}\}$. We solve cut equations in terms of these variables, as we will see later. In $d=4-2\epsilon$, the solution to the cut equations is unique in terms of the ISP, whereas in d=4 we usually have disjoint branches, see double box for an explicit example. \rightarrow Badger, Simon and Frellesvig, Hilatte and Zhang, Yang, hep-ph:1202.2019

→ Kosower, David A. and Larsen, Kasper J., hep-th:1108.1180



The parametrization of the polynomials P in terms of the ISP is obtained through the program BasisDet. The latter provides a set of monomials which take the form $\prod_i x_i^{r_i}$, where x_i denote ISP and r_i is an integer ranging from zero to some upper value calculated from the maximal tensor rank of the polynomial P with respect to k_1 , k_2 and k_1 , k_2 combined. \rightarrow Zhane, Yang, hep-ph:1205.5707

At one loop, *P* consists of terms depending solely on the external kinematics and the so-called spurious terms, which are specific to each cut. The spurious terms, although necessary for the reduction at the integrand level, do not contribute to the final result as they integrate to zero. The final result is determined by the coefficients that depend only on the external kinematics and multiply the appropriately chosen basis of integrals. At two loops, the existence of spurious terms that integrate to zero is less straightforward: there are certainly spurious terms compiled by the loop momenta and the transverse directions over the external momenta, whenever present. Nevertheless, the simple one-loop picture is spoiled by the fact that the integrals in Eq. (3) obey a set of IBP identities, resulting in a set of master integrals, which are then evaluated using different techniques.

Returning to the solution of Eq. (1), let us first address the case of $d=4-2\epsilon$ dimensions. The cut equations fix a subset of the eleven parameters needed to fully describe the loop momenta. Assuming that the set of monomials m_i $(i=1,\ldots,M)$ parametrizing a given polynomial P is established, then an $M\times M$ matrix, \mathcal{M} , is obtained by evaluating the monomials on the solution to the cut equation, by assigning M random values to the free parameters of the vector \vec{X} , obtaining thus M instances of it, i.e. \vec{X}_j , $j=1,\ldots,M$, and then computing the elements of the matrix \mathcal{M} , as follows: $\mathcal{M}_{i,j}\equiv m_i(\vec{X}_j)$. The numerator $\mathcal{N}(\vec{X},d)$ can be cast in the form

$$\mathcal{N} \equiv \mathcal{N}(\vec{X}, d) = \mathcal{N}_0 + \sum_{i>1} \epsilon^i \mathcal{N}_{\epsilon}^{(i)}, \qquad (9)$$

by expanding in powers of $\epsilon \equiv (4-d)/2$, where both $\mathcal{N}_0 \equiv \mathcal{N}(\vec{X},d)|_{d=4}$ and $\mathcal{N}_{\epsilon}^{(i)} \equiv \mathcal{N}_{\epsilon}^{(i)}(\vec{X})$, are accessible numerically and depending on μ_{ij} through \vec{X} . These terms are used to calculate, the $M \times 1$ matrices, $\mathcal{B}_j^{(0)} = \mathcal{N}_0(\vec{X}_j)$, $\mathcal{B}_j^{(i)} = \mathcal{N}_{\epsilon}^{(i)}(\vec{X}_j)$. Then the given polynomial P is written explicitly as

$$P = \sum_{i=1}^{M} \left(c_i^{(0)} + \sum_{i} \epsilon^j c_i^{(j)} \right) m_i \tag{10}$$

where

$$\vec{c}^{(0)} = \mathcal{M}^{-1} \mathcal{B}^{(0)} \qquad \vec{c}^{(i)} = \mathcal{M}^{-1} \mathcal{B}^{(i)}$$
 (11)

After the whole iterative procedure is completed, the so-called N=N test is performed. The latter consists of checking the validity of Eq. (1) for arbitrary assignment of numerical values for all free parameters of the loop kinematics, \vec{X} , not restricted by cut equations. We have checked that the N=N test is fulfilled when the polynomials P are constructed directly from the analytic expression of the numerator, as well as when using BasisDet to construct the ansatz for the polynomials.

In d=4 we obtain several disjoint solutions of the cut equations in terms of $\vec{X}^{(d=4)}=\{x_1,x_2,x_3,x_4,y_1,y_2,y_3,y_4\}$. On each branch, we have checked analytically that the d=4 numerator, $\mathcal{N}_{4,0}\equiv\mathcal{N}(\vec{X},d)|_{\mu_{ii}=0,d=4}$, assumes a different form. On the other hand, the set of monomials obtained previously in $d=4-2\epsilon$ dimensions, contains linear dependencies due to the fact that in d=4 the two loop momenta and the three independent external momenta, in a 4-particle amplitude for instance, is an over complete set and Gram determinants among them vanish, leading to non-trivial relations. In that case, the set of monomials m_i , $i=1,\ldots,M$, provided by BasisDet, is evaluated at each branch of the cut-equation solution. Assuming the existence of r branches, the matrix \mathcal{M} of size $(rM) \times M$ and the matrix $\mathcal{B}_0^{(4)}$ of size $(rM) \times 1$, are calculated using $\mathcal{M}_{i..i} \equiv \textit{m}_{i}(\vec{X}_{i}^{(d=4)}), \; \mathcal{B}_{\text{D}i}^{(4)} \equiv \mathcal{N}_{4,0}(\vec{X}_{i}^{(d=4)}), \; \text{with} \; i=1,\ldots,M, \; j=1,\ldots,rM. \; \text{The system}$

$$\mathcal{M}\vec{c}^{(d=4)} = \mathcal{B}_0^{(4)}$$
 (12)

can still be solved with standard Linear Algebra algorithms such as QR decomposition, as long as the rank of the matrix is full, namely $rank(\mathcal{M}) = M$. As we will see later, this is true in most cases, but solutions can still be obtained in cases where the matrix is rank-deficient, $rank(\mathcal{M}) < M$. Notice that in $d = 4 - 2\epsilon$ case, when the information on the dependence of the numerator on d and μ_{ii} is available, the reduction of the amplitude is complete, whereas in four dimensions, where this information is not available, the so-called rational terms need to be calculated in addition

> → Ossola, Giovanni and Papadopoulos, Costas G. and Pittau, Roberto, hep-ph: 0806.4600 → Badger, S. D., hep-ph:0802.1876

→ Pozzorini, Stefano and Zhang, Hantian and Zoller, Max F., hep-ph; 2001.11388

Projecting over a full family

From the perspective of the one-loop OPP approach, Eq. (1) addresses the reduction of the numerator in Eq. (1) in terms of the n inverse propagators D_i appearing in it. As we already pointed out, the one-loop case is special in the sense that the number of independent scalar products N and the number of inverse propagators n obey the relation $N \le n$. Thus, all scalar products can be expressed in terms of the D_i 's, which appear in the denominator of the loop integrand. Starting from two loops, N > n, and thus one is left with a set of ISP that cannot be expressed as above. However, one can define an enlarged set of inverse propagators such that all scalar products are expressible as combinations of the latter. This enlarged set of inverse propagators is named family. We can consider projecting the numerator over the full family of inverse propagators:

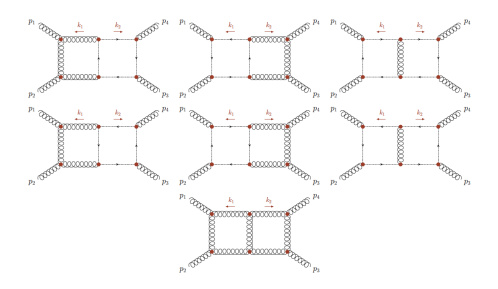
$$\mathcal{N} = P^{(N)} + \sum_{i=1}^{N} P_i^{(N-1)} D_i + \sum_{i=1}^{N-1} \sum_{i>i}^{N} P_{ij}^{(N-2)} D_i D_j + \dots + P_{12...N}^{(0)} D_1 D_2 \dots D_N$$
(13)

APPLICATION OF THE METHOD

The considered numerators are representative of a variety of scattering processes and consist of different kinematic dependencies, ranging from four-point to six-point kinematics. For the generation of the analytic expressions required, we used the Mathematica packages FeynArts and FeynCalc, except for the 6-particle case, which has been generated by FORM.

APPLICATION OF THE METHOD - DOUBLE BOX

Here we focus on the numerator of the double-box topology constructed by the seven Feynman graphs depicted above. This numerator contributes to the scattering amplitude of the process gg o gg.



APPLICATION OF THE METHOD - DOUBLE BOX

The inverse propagators describing the family for this topology can be chosen as

$$D_{1} = k_{1}^{2}, \quad D_{2} = (k_{1} + \rho_{1})^{2}, \quad D_{3} = (k_{1} + \rho_{12})^{2}, \quad D_{4} = (k_{1} + k_{2})^{2}, \quad D_{5} = k_{2}^{2},$$

$$D_{6} = (k_{2} - \rho_{123})^{2}, \quad D_{7} = (k_{2} - \rho_{12})^{2}, \quad D_{8} = (k_{2} - \rho_{1})^{2}, \quad D_{9} = (k_{1} + \rho_{123})^{2}$$
(14)

Above and henceforth, the shorthand notation $p_{i...j} = p_i + ... + p_j$ will be used to denote the sum of the incoming external on-shell momenta, and $s = (p_1 + p_2)^2$ and $t = (p_2 + p_3)^2$ the standard Mandelstam variables

OPP@2L WITH HELAC: LINEAR FIT

The maximal cut equations

$$D_1 = D_2 = D_3 = D_4 = D_5 = D_6 = D_7 = 0 (15)$$

result in determining seven invariants

$$k_1 \cdot k_1 \to 0, \quad k_1 \cdot k_2 \to 0, \quad k_1 \cdot p_1 \to 0, \quad k_1 \cdot p_2 \to -\frac{s}{2}, \quad k_2 \cdot k_2 \to 0,$$

$$k_2 \cdot p_2 \to \frac{s}{2} - k_2 \cdot p_1, \quad k_2 \cdot p_3 \to -\frac{s}{2}.$$
(16)

By applying the above relation on both sides of the master equation, we can fully determine the polynomial P_7 . The latter consists of 70 coefficients over the ISP monomials $\{k_1 \cdot p_3, k_1 \cdot \eta, k_2 \cdot p_1, k_2 \cdot \eta\}$. Subtracting P_7 in the master equation, we can now determine the polynomials of kind P_6 in the same way. There are seven six-cuts and therefore seven P_6 polynomials to determine. As an example, the first six-cut,

$$D_2 = D_3 = D_4 = D_5 = D_6 = D_7 = 0 (17)$$

leads to

$$k_2 \cdot p_2 \to \frac{s}{2} - k_2 \cdot p_1, \quad k_1 \cdot p_2 \to -\frac{s}{2}, \quad k_2 \cdot p_3 \to -\frac{s}{2},$$

$$k_1 \cdot k_2 \to k_1 \cdot p_1, \quad k_1 \cdot k_1 \to -2k_1 \cdot p_1, \quad k_2 \cdot k_2 \to 0,$$
(18)

where there are now 5 ISP: $\{k_1 \cdot p_2, k_1 \cdot p_3, k_1 \cdot \eta, k_2 \cdot p_1, k_2 \cdot \eta\}$. The polynomial $P_1^{(6)}$ consists of 111 coefficients. This process is iterated until the level of a two-cut, after which all resulting polynomials vanish.

The data for all cuts are summarized in Tab. 2. The analytic solution for the polynomials satisfies explicitly the master equation.

Level	Number of cuts	Number of coefficients	Scaling
7	1	70	4,4,4
6	7	695	3,3,4
5	21	1430	3,3,3
4	35	1017	2,2,2
3	35	225	1,1,1
2	21	9	0,0,0

TABLE: Double-box linear fit information beginning with 7-cut. The numbers in the last column refer to the maximum powers of k_1 , k_2 , and k_1 , k_2 combined, as described in the text.

We now seek to solve the master equation, namely projecting over all 9 propagators in the double-box family. This has the advantage of building a reduction procedure that covers all 4-particle planar diagrams, including the double-box, the penta-triangle and the hexa-bubble. The maximal cut equations read

$$D_1 = D_2 = D_3 = D_4 = D_5 = D_6 = D_7 = D_8 = D_9 = 0$$
 (19)

which leads to

$$k_1 \cdot k_1 \to 0, \quad k_1 \cdot k_2 \to 0, \quad k_1 \cdot p_1 \to 0, \quad k_1 \cdot p_2 \to -\frac{s}{2}, \quad k_1 \cdot p_3 \to \frac{s}{2},$$

$$k_2 \cdot k_2 \to 0, \quad k_2 \cdot p_1 \to 0, \quad k_2 \cdot p_2 \to \frac{s}{2}, \quad k_2 \cdot p_3 \to -\frac{s}{2}$$
(20)

By applying the above relations on both sides of the master equation, we can fully determine the polynomial P_0 . The latter consists of 13 coefficients over the ISP monomials $\{k_1 \cdot \eta, \ k_2 \cdot \eta\}$. Subtracting as before P_0 , we can now determine the polynomials P_0 in the same way. There are nine 8-cuts and therefore nine P_0 polynomials to determine. As an example, the first 8-cut,

$$D_2 = D_3 = D_4 = D_5 = D_6 = D_7 = D_8 = D_9 = 0$$
 (21)

leads to

$$k_2 \cdot p_1 \to 0, \quad k_2 \cdot p_2 \to \frac{s}{2}, \quad k_1 \cdot p_2 \to -\frac{s}{2}, \quad k_2 \cdot p_3 \to -\frac{s}{2}, \quad k_1 \cdot p_3 \to \frac{s}{2},$$

$$k_1 \cdot k_2 \to k_1 \cdot p_1, \quad k_1 \cdot k_1 \to -2k_1 \cdot p_1, \quad k_2 \cdot k_2 \to 0.$$
(22)

where there are now 3 ISP: $\{k_1 \cdot p_1, k_1 \cdot \eta, k_2 \cdot \eta\}$.



Level	Number of cuts	Number of coefficients	Scaling
9	1	13	4,4,4
8	9	227	4,4,4
7	36	963	3,3,3
6	84	1445	2,2,2
5	126	780	1,1,1
4	126	116	0,0,0

TABLE: Double-box linear fit information beginning with 9-cut.

The data for all cuts are summarized in Tab. 3. The analytic solutions for the polynomials satisfy explicitly the master equation. The total number of non-zero coefficients is slightly larger than previously, namely 3544 versus 3446. We have verified that after reducing by IBP identities the integrals appearing in the previous equations, the coefficients of the top-sector master integrals coincide with those obtained from Caravel, for all helicity assignments.

 \rightarrow In Caravel the results are given for the color-stripped helicity amplitude, whereas in our case we have studied a subset of the contributions to the amplitude. Nevertheless, a comparison of the top-sector master integral coefficients is possible since all other Feynman graphs do not contribute to them.

→ Abreu, S. and Dormans, J. and Febres Cordero, F. and Ita, H. and Kraus, M. and Page, B. and Pascual, E. and Ruf, M.S. and Sotnikov, V.,

CPC,267(2021),108069.

Fit by cut in $d=4-2\epsilon$ dimensions

Let us now assume that the numerator is available only using a numerical approach, as the one implemented in HELAC-2L00P, including terms proportional to μ_{ij} and $\epsilon = (d-4)/2$. Then the realization of the solutions of the cut equations, Eq. (16) in a numerical setup is based on the determination of the four-dimensional part of the loop momenta following Eq. (8). In fact the solution for any cut has a unique analytic form in terms of ISP. The 7 cut, Eq. (16), reads as follows:

$$k_{1} \cdot \rho_{1} \to 0, \quad k_{2} \cdot \rho_{2} \to \frac{1}{2} \left(s - 2k_{2} \cdot \rho_{1} \right), \quad k_{1} \cdot \rho_{2} \to -\frac{s}{2}, \quad k_{2} \cdot \rho_{3} \to -\frac{s}{2},$$

$$\mu_{11} \to -\frac{\frac{4s\left(k_{1} \cdot \rho_{3}\right)^{2}}{s+t} - 4sk_{1} \cdot \rho_{3} + 4t\left(k_{1} \cdot \eta\right)^{2} + s\left(s + t\right)}{4t},$$

$$\mu_{12} \to \frac{\frac{k_{1} \cdot \rho_{3}\left(4\left(s + 2t\right)k_{2} \cdot \rho_{1} - 2st\right)}{s+t} + t\left(s - 4k_{1} \cdot \eta k_{2} \cdot \eta\right) - 2sk_{2} \cdot \rho_{1}}{4t},$$

$$\mu_{22} \to -\frac{4stk_{2} \cdot \rho_{1} + 4s\left(k_{2} \cdot \rho_{1}\right)^{2} + t\left(4\left(s + t\right)\left(k_{2} \cdot \eta\right)^{2} + st\right)}{4t\left(s + t\right)}$$

$$(23)$$

For comparison, the cut conditions for 9 propagators, Eq. (20), are

$$k_{2} \cdot p_{1} \to 0, \quad k_{1} \cdot p_{1} \to 0, \quad k_{2} \cdot p_{2} \to \frac{s}{2}, \quad k_{1} \cdot p_{2} \to -\frac{s}{2},$$

$$k_{2} \cdot p_{3} \to -\frac{s}{2}, \quad k_{1} \cdot p_{3} \to \frac{s}{2}, \quad \mu_{11} \to -(k_{1} \cdot \eta)^{2} - \frac{st}{4(s+t)},$$

$$\mu_{12} \to \frac{st}{4(s+t)} - k_{1} \cdot \eta k_{2} \cdot \eta, \quad \mu_{22} \to -(k_{2} \cdot \eta)^{2} - \frac{st}{4(s+t)}$$
(24)

In terms of the basis introduced before, i.e. $\{x_1,\ldots,x_4,y_1,\ldots,y_4,\mu_{11},\mu_{12},\mu_{22}\}$, the solution takes the form

$$x_1 \to -1$$
, $x_2 \to 0$, $y_1 \to 0$, $y_2 \to -1$, $\mu_{11} \to 4sx_3x_4$, $\mu_{22} \to 4sy_3y_4$,
 $\mu_{12} \to (x_3 + x_4 - y_3 - y_4)r - 2(s + t)(x_4y_4 + x_3y_3) - 2t(x_3y_4 + x_4y_3) - t/2$
(25)

with $r = \sqrt{-t(s+t)}$. In a numerical setup, for instance, calculating on the kinematic point s = 1, t = -1/5, the 7-cut is represented by

$$x_1 \to -1$$
, $x_2 \to 0$, $y_1 \to 0$, $y_2 \to -1$, $\mu_{11} \to 4x_3x_4$, $\mu_{22} \to 4y_3y_4$,
 $\mu_{12} \to (4x_3(-4y_3 + y_4 + 1) + 4x_4(y_3 - 4y_4 + 1) - 4y_3 - 4y_4 + 1)/10$ (26)

We can now determine the coefficients of the polynomial P_7 , which in this case has 70 coefficients, by calculating the numerator \mathcal{N} , and the monomials m_i of the basis, using 70 random assignments of the undetermined variables, x_3, x_4, y_3, y_4 , *i.e.* \mathcal{N}_i and M_{ij} respectively, and solving the corresponding matrix equation

$$\sum_{j=1}^{70} M_{ij} c_j = \mathcal{N}_i, \quad i = 1, \dots, 70$$
 (27)

for the unknown coefficients c. The full-rank matrix M is straightforwardly invertible, and the solution checked agrees to the numerical precision used against the analytic result. We have confirmed that this way we can calculate all the coefficients of Tab. 2 numerically. The same is true for the case of projecting over the 9 propagators, see Tab. 3.

FIVE-POINT KINEMATICS/PENTA-BOX TOPOLOGIES

Here we consider the numerator of the penta-box topology constructed by the seven Feynman graphs depicted below, which contributes to the scattering amplitude of the process $gg \to ggg$.

FIVE-POINT KINEMATICS/PENTA-BOX TOPOLOGIES

$$D_{1} = k_{1}^{2}, \quad D_{2} = (k_{1} + \rho_{1})^{2}, \quad D_{3} = (k_{1} + \rho_{12})^{2}, \quad D_{4} = (k_{1} + k_{2})^{2},$$

$$D_{5} = k_{2}^{2}, \quad D_{6} = (k_{2} - \rho_{1234})^{2}, \quad D_{7} = (k_{2} - \rho_{123})^{2}, \quad D_{8} = (k_{2} - \rho_{12})^{2},$$

$$D_{9} = (k_{1} + \rho_{123})^{2}, \quad D_{10} = (k_{1} + \rho_{1234})^{2}, \quad D_{11} = (k_{2} - \rho_{1})^{2}$$
(28)

The external kinematics is described by 4 independent momenta and five independent invariants, which can be chosen to be $S_5 = \{s_{12}, s_{23}, s_{34}, s_{45}, s_{15}\}$, where $s_{ij} = (p_i + p_j)^2$. In order to proceed with the reduction in an analytic setup, the expression of the numerator needs to be expressed in terms of the 11 invariants V_{11} , defined as the set of variables $k_i \cdot k_j$, with i, j = 1, 2, and $k_i \cdot p_j$ with $i = 1, 2, j = 1, \ldots, 4$. Since the analytic expression of the numerator involves the polarization vectors of the external gluons, ε_i , $i = 1, \ldots, 5$, scalar products of the form $k_i \cdot \varepsilon_j$ need to be expressed in terms of the set of variables S_5 and V_{11} . To this end, the following relation is used

$$q_i \cdot q_j = G_{kl}^{-1} q_i \cdot p_k q_j \cdot p_l \tag{29}$$

where q_i stands for any momentum or polarization vector and G denotes the Gram matrix, $G_{ij}=p_i\cdot p_j, i,j=1,\ldots,4$ expressed in terms of the S_5 variables. Barring that the analytic expression for the inverse Gram matrix and the numerator are complicated expressions, it is convenient to work in a numerical setup, using exact arithmetic. The numerical values for the variables S_5 , are chosen as $\left\{s_{12} \to 1, s_{34} \to \frac{1}{4}, s_{45} \to \frac{1}{4}, s_{15} \to -\frac{1}{4}, s_{23} \to -\frac{1}{8}\right\}$. The polarization vectors are defined by

$$\varepsilon_{\mu}^{+}(\rho_{i}) = \frac{1}{\sqrt{2}\bar{u}_{-}(\rho_{i+1})u_{+}(\rho_{i})}\bar{u}_{-}(\rho_{i+1})\gamma_{\mu}u_{-}(\rho_{i}) \quad \varepsilon_{\mu}^{-}(\rho_{i}) = -\frac{1}{\sqrt{2}\bar{u}_{+}(\rho_{i+1})u_{-}(\rho_{i})}\bar{u}_{+}(\rho_{i+1})\gamma_{\mu}u_{+}(\rho_{i}) \quad (30)$$

for $i=1,\ldots,5$, where in the above formula the following the $p_6\to p_1$ identification is assumed. With the above identifications, the numerator consists of monomials composed of the V_{11} variables, with exact numerical coefficients.

4 D > 4 A > 4 B > 4 B > B = 900

The maximal cut is given by

$$k_1 \cdot k_1 \to 0, \quad k_1 \cdot k_2 \to 0, \quad k_1 \cdot p_1 \to 0, \quad k_1 \cdot p_2 \to -\frac{s_{12}}{2}, \quad k_2 \cdot k_2 \to 0,$$

$$k_2 \cdot p_2 \to \frac{s_{12}}{2} - k_2 \cdot p_1, \quad k_2 \cdot p_3 \to \frac{s_{45}}{2} - \frac{s_{12}}{2}, \quad k_2 \cdot p_4 \to -\frac{s_{45}}{2}$$
(31)

The P_8 polynomial consists of 50 terms, composed of monomials in the ISP variables $\{k_1 \cdot p_3, k_1 \cdot p_4, k_2 \cdot p_1\}$. By following the usual subtraction procedure the data of this solution are given in Tab. 4.

Level	Number of cuts	Number of coefficients	Scaling
8	1	50	4,5,5
7	8	705	4,4,5
6	28	2550	4,4,4
5	56	3508	3,3,3
4	70	1902	2,2,2
3	56	348	1,1,1
2	28	12	0,0,0

TABLE: Penta-box linear fit information beginning with 8-cut.

Seeking now to solve Eq. (??) the maximal cut is given by

$$k_1 \cdot k_1 \to 0, \quad k_1 \cdot k_2 \to 0, \quad k_1 \cdot p_1 \to 0, \quad k_1 \cdot p_2 \to -\frac{s_{12}}{2}, \quad k_1 \cdot p_3 \to \frac{s_{12}}{2} - \frac{s_{45}}{2},$$

$$k_1 \cdot p_4 \to \frac{s_{45}}{2}, \quad k_2 \cdot k_2 \to 0, \quad k_2 \cdot p_1 \to 0, \quad k_2 \cdot p_2 \to \frac{s_{12}}{2},$$

$$k_2 \cdot p_3 \to \frac{s_{45}}{2} - \frac{s_{12}}{2}, \quad k_2 \cdot p_4 \to -\frac{s_{45}}{2}$$
(32)

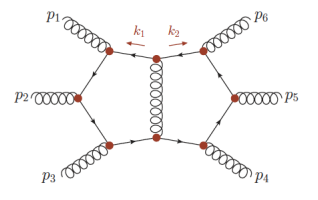
and as before, the cut data are shown in Tab. 5.

Level	Number of cuts	Number of coefficients	Scaling
11	1	1	0,0,0
10	11	47	3,4,4
9	55	502	3,4,4
8	165	2313	3,3,3
7	330	3715	2,2,2
6	462	2255	1,1,1
5	462	425	0,0,0

TABLE: Penta-box linear fit information beginning with 11-cut.

SIX-POINT KINEMATICS/SIX-GLUON TOPOLOGY

In this subsection, we apply our method to the case of the six-gluon two-loop numerator topology. This graph is part of the gg o gggg scattering amplitude.



We define the propagators of the family in which this topology belongs, as

$$\begin{split} D_1 &= k_1^2, \quad D_2 = (k_1 + p_1)^2, \quad D_3 = (k_1 + p_{12})^2, \quad D_4 = (k_1 + p_{123})^2, \quad D_5 = (k_1 + k_2)^2, \\ D_6 &= k_2^2, \quad D_7 = (k_2 - p_{12345})^2, \quad D_8 = (k_2 - p_{1234})^2, \quad D_9 = (k_2 - p_{123})^2, \\ D_{10} &= (k_1 + p_{1234})^2, \quad D_{11} = (k_1 + p_{12345})^2, \quad D_{12} = (k_2 - p_{12})^2, \quad D_{13} = (k_2 - p_1)^2 \end{split}$$

SIX-POINT KINEMATICS/SIX-GLUON TOPOLOGY

Since out of the six external momenta only four are independent in d=4 dimensions, not all 13 propagators in Eq. (54) are independent. In general, for any n-point amplitude, with $n\geq 5$, only 11 propagators are independent. We have chosen the following subset, $\{D_1,\ldots,D_{10},D_{13}\}$ having expressed p_5 in terms of p_1,\ldots,p_4 through Eq. (29). As in the case of the penta-box, section ??, the analytic expressions are hardly manageable, and it is convenient to work in a numerical setup, using exact arithmetic. The numerical values of the invariants are chosen as 1

$$\left\{s_{12} \to 4, s_{23} \to -1, s_{34} \to 1, s_{45} \to \frac{5}{4}, s_{56} \to \frac{1}{2}, s_{16} \to -1, s_{123} \to 2, s_{234} \to -1, s_{345} \to \frac{31}{12}\right\},$$

with $s_{ijk} = (p_i + p_i + p_k)^2$. For the polarization vectors we follow Eq. (30), with the identification of $p_7 \to p_1$.

The 9-cut

$$D_1=\ldots=D_9=0 \tag{33}$$

is given, in the numerical point chosen, by

$$k_1 \cdot k_1 \to 0, \quad k_1 \cdot k_2 \to 0, \quad k_1 \cdot p_1 \to 0, \quad k_1 \cdot p_2 \to -2, \quad k_1 \cdot p_3 \to 1, \quad k_2 \cdot k_2 \to 0,$$

$$k_2 \cdot p_2 \to \frac{5}{2} - \frac{5k_2 \cdot p_1}{3}, \quad k_2 \cdot p_3 \to \frac{2k_2 \cdot p_1}{3} - \frac{3}{2}, \quad k_2 \cdot p_4 \to -\frac{3}{4}$$
(34)

The reduction data are given in Tab. 6.

Level	Number of cuts	Number of coefficients	Scaling
9	1	21	4,4,6
8	9	355	4,4,6
7	36	1949	4,4,5
6	84	4462	4,4,4
5	126	4540	3,3,3
4	126	2016	2,2,2
3	84	334	1,1,1
2	36	16	0,0,0

TABLE: 6 gluon linear fit information beginning with 9-cut.

Projecting over the set of 11 propagators, referred above, the 11-cut is given by

$$k_1 \cdot k_1 \to 0, \quad k_1 \cdot k_2 \to 0, \quad k_1 \cdot p_1 \to 0, \quad k_1 \cdot p_2 \to -2, \quad k_1 \cdot p_3 \to 1,$$

$$k_1 \cdot p_4 \to \frac{3}{4}, \quad k_2 \cdot k_2 \to 0, \quad k_2 \cdot p_1 \to 0, \quad k_2 \cdot p_2 \to \frac{5}{2},$$

$$k_2 \cdot p_3 \to -\frac{3}{2}, \quad k_2 \cdot p_4 \to -\frac{3}{4}$$
(35)

and the reduction data are summarized in Tab. 7.

Level	Number of cuts	Number of coefficients	Scaling
11	1	1	0,0,0
10	11	41	3,3,3
9	55	505	3,3,5
8	165	2365	3,3,4
7	330	4780	3,3,3
6	462	4290	2,2,2
5	462	1592	1,1,1
4	330	200	0,0,0

TABLE: 6 gluon linear fit information beginning with 11-cut.

OTHER CONTRIBUTIONS

Penta-1	Hexa-bubble	
		今心心心
Non-planar double box	gg o t ar t	gg o t ar t H
		XXX XXX

ightarrow Bevilacqua, Giuseppe and Canko, Dhimiter and Papadopoulos, Costas and Spourdalakis, Aris,, hep-ph: 2506.07231

Mon, October 27

10:00 AM 10:30 AM	Full Classification of Feynman Integral Geometries at Two Loops Contribution Speaker: Hjalte Freiliesvig
10:30 AM 11:00 AM	Frontier of multi-loop multi-leg Feynman integrals Contribution Speaker: Yang Zhang
11:00 AM 11:30 AM	Numerical methods for the evaluation of two-loop master integrals for \$pp \to t \bar(t) j\$ Contribution Speaker Michal Czakon
11:30 AM 12:00 PM	Two-loop integrand reduction Contribution Speaker: Konstantinos Papadopoulos
12:15 PM 12:45 PM	Construction of two-loop amplitudes with HELAC Contribution Speaker: Dhimler Canko
12:45 PM 1:15 PM	Numerical evaluation of dimensionally regularized amplitudes Contribution Speaker: Glusoppe Bevilacqua
1:15 PM 1:45 PM	Numerical implementation of integrand level reduction in HELAC Contribution Speaker: Aris-George-Baidur Spoundalakis
2:30 PM 3:00 PM	Two-loop all-plus helicity amplitudes for self-dual Higgs boson with gluons via unitarity cut constraints Contribution Speaker: Federico Ripani
3:00 PM 3:30 PM	Two-loop Feynman integrals for NNLO QCD corrections to ttW production Contribution Speaker: Mattee Becchetti
3:30 PM 4:00 PM	Integral reduction & differential equations with CALICO Contribution Speaker: Gala Fontana
4:00 PM	Two loop RGEs for Effective Field Theories Contribution Speakers Achillets Lazopoulos

Summary & Outlook

Current:

- ullet Integrand construction @2L ightarrow solved and implemented
- Cut equations @2L: determining on-shell loop momenta → solved, implementation in progress
- Integrand basis construction and fitting @2L → solved, implementation in progress
 →V. Sotnikov, doi:10.6094/UNIFR/151540
- $d=4-2\epsilon o ext{implementation in progress for 1 loop}$

Near future:

- $d=4-2\epsilon o$ to be extended to 2 loops
- IBP reduction tables and MI numerical evaluation

```
→ D. Chicherin and V. Sotnikov, JHEP 20 (2020), 167
```

→D. Chicherin, V. Sotnikov and S. Zoia, JHEP 01 (2022), 096

Next-to-near future: automated 2-loop amplitude evaluation

ACKNOWLEDGING

Thank you for your attention!

The research project was supported by the Hellenic Foundation for Research and Innovation (H.F.R.I.) under the 2nd Call for H.F.R.I. Research Projects to support Faculty Members & Researchers (Project Number: 2674).

